



# Spatio-temporal charging model for the identification of bottlenecks in planned highway charging infrastructure for passenger BEVs

Antonia Golab · Sebastian Zwickl-Bernhard · Theresia Perger · Hans Auer

Received: 26 July 2022 / Accepted: 30 September 2022 / Published online: 23 November 2022  
 © The Author(s) 2022

**Abstract** Fast-charging capacities must be sufficiently allocated to meet the charging demand of the growing battery electric vehicle (BEV) fleet. We present a methodology for testing the implementability of a planned charging infrastructure for highway networks in terms of underutilized charging capacities and bottlenecks. A linear optimization model for determining charging activities at a fast-charging infrastructure was developed to accomplish this. Using a bottom-up approach, we modeled the charging activities based on the traffic flow between starting and destination points in the network. The proposed model is applied to a planned fast-charging infrastructure along the highway network in the east of Austria. The obtained results reveal that the charging infrastructure is capable of meeting demand during all observed extreme traffic load and temperature conditions. Thus, no bottlenecks are detected, but locations of charging stations with overestimated capacities are discovered, implying that the local capacities would never be fully utilized. Our findings also highlight the importance of considering the spatio-temporal dynamics of charging activities and the traffic flow when expanding fast-charging infrastructure.

**Keywords** Spatio-temporal modeling · Fast-charging station placement and sizing · Battery electric vehicles · Austrian high-level road network · Linear optimization model · Testing of infrastructure implementability

**Räumlich-zeitliche Modellierung von Ladeaktivitäten zur Identifizierung von Engpässen in geplanter Autobahnladeinfrastruktur für batterieelektrische PKWs**

**Zusammenfassung** Die Schnellladekapazitäten müssen regelmäßig erweitert werden, um den Ladebedarf der wachsenden Flotte von batterieelektrischen Fahrzeugen zu decken. In dieser Arbeit präsentieren wir eine Methodik, mit der die Umsetzbarkeit einer geplanten Autobahnladeinfrastruktur im Hinblick auf Ladekapazitäten, die kaum genutzt werden, und Engpässe in den Ladevorgängen getestet werden kann. Zu diesem Zweck wurde ein lineares Optimierungsmodell entwickelt, das die Ladeaktivitäten an einer vorgegebenen Schnellladeinfrastruktur modelliert. In dieser Modellformulierung wird ein Bottom-up-Ansatz verwendet, wobei die Ladeaktivitäten basierend auf dem Verkehrsfluss modelliert werden. Das vorgeschlagene Modell wird auf eine geplante Schnellladeinfrastruktur entlang des Autobahnnetzes im Osten Österreichs angewendet. Die Ergebnisse zeigen, dass die betrachtete Ladeinfrastruktur ausreichend ist, um die Nachfrage unter verschiedenen extremen Bedingungen in Bezug auf Verkehrsbelastung und Temperatur zu decken. Daher werden hier keine Engpässe festgestellt, hingegen aber schon Standorte von Ladestationen mit überschätzten Ladekapazitäten entdeckt, d.h. die dort geplanten Kapazitäten würden nie vollständig genutzt werden. Darüber hinaus zeigen unsere Ergebnisse, dass die Beachtung von der räumlich-zeitlichen Dynamik von Ladeaktivitäten und dem Verkehrsfluss den Ausbau der Schnellladeinfrastruktur optimaler gestalten kann.

T. Perger is an OVE member.

A. Golab (✉) · S. Zwickl-Bernhard · T. Perger · H. Auer  
 Energy Economy Group (EEG), TU Wien,  
 Gusshausstraße 25–29, E370-3, 1040 Vienna, Austria  
[golab@eeg.tuwien.ac.at](mailto:golab@eeg.tuwien.ac.at)

**Schlüsselwörter** Räumlich-zeitliche Modellierung · Platzierung und Dimensionierung von Schnellladestationen · Batterieelektrische Fahrzeuge · Österreichisches hochrangiges Straßennetz · Lineares Optimierungsmodell · Prüfung der Implementierbarkeit von Infrastruktur

## 1 Introduction

The Paris Agreement stipulates a clear goal for the electrification of the passenger transport sector for 2040, implying that 20% of the global passenger transport fleet must be electrified by that time. Following such stipulation, many countries have committed to meeting these goals and motivating the diffusion of battery electric vehicles (BEVs) by introducing both monetary and non-monetary incentives [6, 28, 32]. Studies that have analyzed barriers and effective motivators for the adoption of BEVs have identified that fast-charging plays a critical role [3, 6]. They find that the issue of slow charging causing aversion to purchasing a BEV can be eliminated by increasing charging power and allocating fast-charging stations in places that are easily accessible to potential BEV drivers.

During the last decade, major advances in the field of BEV technology have been made, and the charging power of a regular BEV has increased significantly, allowing to charge for a distance of 200 km in 15 min (at 150 kW), in contrast to the minimum of one hour (at 22 kW), which is typical for car models introduced to the market at earlier stages of BEV adoption [29]. Following these developments in charging power and growth of the BEV fleet, many countries have established a fast-charging infrastructure, which is expanding rapidly to meet the growing fast-charging demand [28]. Studies on this topic generally distinguish between the development of fast-charging infrastructure in urban areas, rural areas, and high-level road networks. Fast-charging infrastructure planning along highway and motorway networks<sup>1</sup> stands out here because of the less flexible route choice. Planning of charging capacities for highway networks mainly focus on the allocation of charging stations at a sufficient density to counteract range anxiety<sup>2</sup> and sizing these charging stations to meet the local charging demand while avoiding waiting times of the BEV drivers [26].

Many studies have proposed methodologies for charging infrastructure planning [23, 26]. Most of these studies modeled an initial setup of charging infrastructure, focusing exclusively on determining the optimal positions for the charging stations [7,

19]. Others also plan the sizing of the charging stations [20, 34]. Nonetheless, many of the proposed methodologies, make various assumptions and simplifications related to charging demand estimation. Given this, tools are required to determine which planning approach to use and which planned charging infrastructure to implement to ensure adequate coverage of charging demand coverage while also allocating investment costs in charging infrastructure cost-effectively.

This paper's work is concerned with this specific problem statement. We propose a modeling framework for testing the feasibility of a planned fast-charging infrastructure. We accomplish this by modeling charging activity using a bottom-up approach with the charging activity based on traffic flow movement. The modeling framework is applied to a planned fast-charging infrastructure along the highway network in the east of Austria for 2030. This charging infrastructure is tested under different realistic conditions and charging demand distributions. The primary goals are to identify potentially missallocated or missing charging capacities and to derive implications for the design of planning tools for future highway charging infrastructure expansion.

## 2 Literature Review

### 2.1 Charging infrastructure planning models for high-level road networks

[23] examined the various proposed models designed to plan BEV charging infrastructure. The modeling approaches used differ significantly in terms of the input variables considered and the output type; for example, although some model types only decide on the allocation of charging infrastructure, others also determine the optimal sizing of charging stations. The authors of [23] identify that the most frequent approach in the optimization of fast-charging infrastructure for highway networks is the flow-capturing location model (FCLM), which was originally introduced by [17] and is formulated as a mixed-integer linear program (MILP). The most important input data for this are the information on origin-destination traffic flows, which describe the total number of vehicles traveling between network nodes in a single day. Accordingly, a predetermined number of charging stations are assigned to potential positions for charging station placement while maximizing the number of vehicles passing these. Some studies propose extensions: The flow-refueling location model (FRLM) [21] and the capacitated FRLM (CFRLM) [33] are two notable extensions. The former formulation considers the vehicles' limited range, whereas the latter succeeds in including constraints that impose an upper limit on charging capacity at a charging station. The authors of [35] present a planning tool for the long-term charging infrastructure planning. This planning

<sup>1</sup> In this work, highways and motorways are included in the term *highway*.

<sup>2</sup> *Range anxiety* describes the fear of being stranded while traveling with a BEV due to the limited driving range of the vehicle and unavailability of a charging opportunity.

tool is based on the FCLM and considers changes in traffic flows, BEV technology, and the user's costs over time. In the study of [36] where the allocation and sizing of charging stations is optimized in two steps, the FRLM is used to first determine the optimal allocations. In the second step, the local charging capacities are determined by simulating vehicle flow along the highway network to estimate the charging demand at each charging station.

Other planning approaches, in addition to the widely used FCLM, can be found in the literature: For example, in [25], an iterative approach based on graph analysis is described which determines the optimal number of charging points at highway service areas. In [10], a MILP model with nonlinear constraints is formulated. This model formulation considers traffic movement and queuing processes in great detail, and the objective function incorporates the minimization of queuing times at charging stations. Meanwhile, in the study [11], charging demand is first approximated for each service area based on the local traffic count. Given the limited driving range of BEVs and the limited number of charging points in a service area, a cost-effective demand-covering charging infrastructure is designed.

## 2.2 Modeling charging activity based on spatial and temporal traffic flow dynamics

Charging activity is frequently modeled to plan the charging infrastructure or the distribution grid [8, 18, 36]. Although some studies derive the geographical distribution of charging demand using information about typical mobility patterns [24, 31], others obtain time series on charging activity in spatial and temporal extent based on traffic flow modeling: In the above-mentioned study by [36], the movement of singular vehicles is simulated and for each, the position of where they charge is determined based on a fixed set of charging station allocations. [2] represent traffic flow and charging activities along highways using the fluid dynamic model. The model formulation includes a predetermination of the number of vehicles needing to charge at a given charging station and the assumption that vehicles will only charge once during a trip. [39] propose modeling charging demand using the cell transmission model and develop an urban charging demand model. Cells in their model formulation represent nodes, and charging stations. The number of vehicles entering a charging station is counted for each cell. Moreover, the number of vehicles entering a charging station is determined by an assumed ratio of vehicles passing a charging station and the ones entering to charge.

## 2.3 Testing implementability of planned charging infrastructure

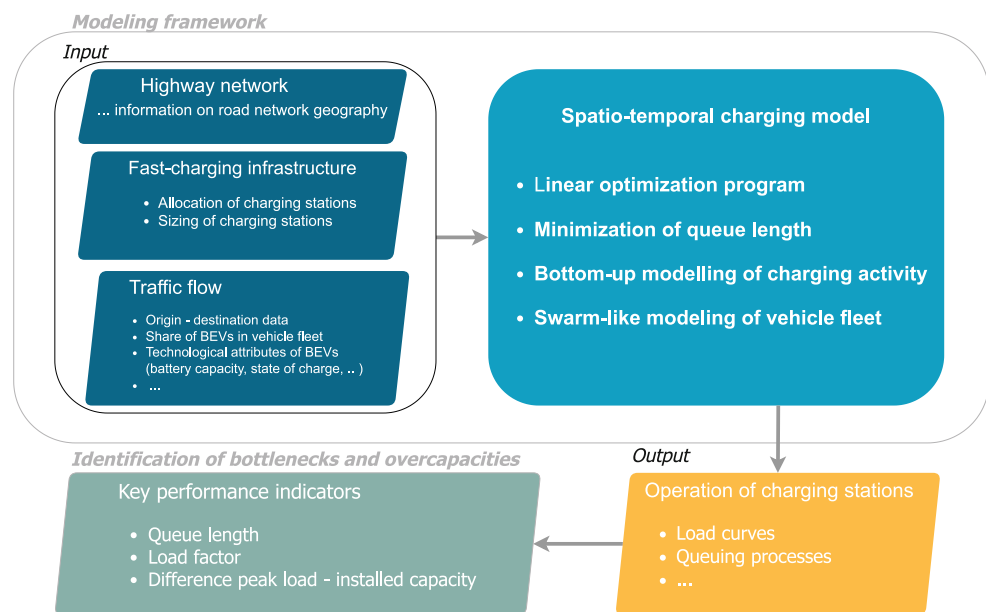
In scientific literature, the testing of the implementability of infrastructure that is planned by various types of planning tools is rich in the field of energy systems and transport [13, 37]. However, research that is particularly dedicated to the testing of charging infrastructure is scant. In particular, only two studies of this kind are found in the literature. In the study by [22], an agent-based simulation is used to identify bottlenecks in charging stations that are allocated at workplaces. The charging processes are modeled in great detail, with the model incorporating, for example, the process of cable switching at a charging pole. The charging demand is modeled using typical community mobility patterns. All vehicles are plug-in hybrid electric vehicles, and bottlenecks are identified based on the e-mileage of the hybrid vehicles. [15] present an agent-based simulation to stress-test urban fast-charging infrastructure. This research aims to gain insight into strategies for the optimal expansion of public fast-charging infrastructure. The authors use key performance metrics such as the occupancy ratio and the frequency of failed charging attempts to identify allocations of missing charging capacities.

## 2.4 Progress beyond state of the art:

Based on this literature review, the scientific contribution and novelties of this work can be summarized as follows:

- With this study, we contribute to the currently scarce collection of studies dedicated to the stress-testing of charging infrastructure. The current study is the first one explicitly dedicated to the application of fast-charging infrastructure along highway networks in this context. Numerous proposed methods exist for planning and expanding charging infrastructure, and the growing share of BEVs necessitates their implementation. Therefore, the implementability of a planned charging infrastructure must be validated and tested to ensure that the installed charging stations and their sizing meet the charging demand while ensuring cost-effective allocation of infrastructure investment costs.
- We develop a charging model that determines the queuing and charging activities in a given fast-charging infrastructure. The model is formulated as a linear optimization program. Vehicle fleets are modeled as continuous, swarm-like entities in this model, resulting in a coarser granularity to the representation of traveling vehicles than in agent-based models. This allows the identification of infrastructural bottlenecks at geographically wider scale.

**Fig. 1** Modeling framework and derived key performance indicators for testing the implementability of a planned charging infrastructure



- The focus of this study is not only identifying missing or overestimated charging infrastructure capacities, but also on determining implications for improving the fast-charging infrastructure planning. The wide range of proposed modeling approaches used in the planning of highway charging infrastructure differ in the mathematical formulation, considered input parameters, and assumptions made in their design. Given this, the question arises as to what degree of limited input information, considering traffic flow, mobility patterns, and related assumptions, still leads to a sufficient allocation of charging capacity.

### 3 Methodology and Materials

The modeling framework's design aims to test the implementability of a planned fast-charging infrastructure. This includes, on the one hand, determining whether charging demand is sufficiently covered without significantly prolonging trips by long-distance travelers<sup>3</sup> driving a BEV, that is, identifying the presence of potential bottlenecks, and, on the other hand, testing whether the charging infrastructure is cost-efficiently allocated, so that no overcapacities are installed that are never used – this would indicate a poor allocation of investment costs in charging infrastructure. The outline of this modeling framework is illustrated in Fig. 1:

- The **spatio-temporal charging model** forms the key component of this modeling framework. The model maps charging activity at charging stations in both time and space. This is accomplished by considering the spatial and temporal dimensions of traffic

load along the highway network, including origin-destination flows and mapping charging demand bottom-up. The model is formulated as a linear optimization model, with continuous, swarm-like entities representing the traveling vehicle fleet along the highway network. The objective function describes the minimization of the number of waiting vehicles at all charging stations which directly minimizes the amount of time spent waiting at charging stations during all trips conducted on the given highway network.

- One part of the **input data** for the optimization model is the geography of the highway network along with information on the planned charging infrastructure for this network. The required descriptors of this input are, in particular, the locations of fast-charging stations and their respective sizing, that is, the planned capacities at each charging station. Furthermore, the number of traveling BEVs between specific origin and destination points, as well as the state of charge of the vehicles at the time of entry into the highway network are part of the traffic flow data. Both these parameters are determined randomly for each highway-entering vehicle fleet to include a representation of the variability of the vehicles' state of charge.
- The most relevant **output data** of the optimization model used for further analysis are the load curves describing the operation of each charging station and time series reflecting the number of vehicles waiting in the queue to charge.
- To assess the implementability of the planned charging infrastructure, this study derived **key performance indicators (KPIs)** from the output data of the optimization model. At all planned charging stations, three KPIs are determined: The number of waiting vehicles in a queue corresponds to the

<sup>3</sup> Travelers with a trip distance of at least 100 km [9].



number of vehicles whose charging demand is met with a delay rather than immediately upon arrival at a charging station. While queue length aids in the identification of bottlenecks in the charging infrastructure, two technical parameters, namely, the utility rate and the difference between planned capacities and the peak power at which a charging is operated, are also introduced as KPIs. These two KPIs are intended to provide insights into the business case of a fast-charging station along a highway, and reveal planned capacities that would be rarely or never used.

### 3.1 Spatio-temporal charging model

The spatio-temporal charging model is formulated as a linear optimization program. Vehicles are accumulated to fleets  $f$  and modeled as a swarm-like entity. This grouping is made by accumulating vehicles driving a similar route, that is, traveling among the same highway sections  $c$ . Each fleet's movement and charging activity is observed at time steps  $t \in \mathcal{T}$  which are set after a chosen time resolution  $\Delta t$ . The extend of a highway section  $c$ ,  $dist_c$ , is directly defined by  $\Delta t$  via  $dist_c = \Delta t * v_c$ ,  $v_c$  being the average driving speed within the highway section  $c$ . Based on a given charging infrastructure, a charging capacity of the size  $Cap_c$  is assigned to highway sections at which charging stations are allocated.

To implement the BEV drivers desire of avoiding queues, the following objective function is formulated:

$$\min_x \sum_f \sum_c \sum_t n_{f,c}^{queue,t} \quad (1)$$

This expresses the minimization of the number of vehicles waiting in queue,  $n_{f,c}^{queue,t}$  of all fleets  $f$  at all highway sections  $c$  and at all observed time steps  $t^t$ . The objective function introduces a fundamental assumption in this model formulation: highway charging is coordinated. BEV drivers would always charge in such a way – in terms of location and timing – that the total number waiting vehicles of all traveling vehicles on the highway network is kept to a minimum.

<sup>4</sup> Note that this representation of the queuing process is different from the traditional representations such as the M/M/\* model that allows to express the uncertainty of the arrival moment at a service area. We do not explicitly consider uncertainty in this case because the departure time is determined randomly. Furthermore, the discrete queue representation used here allows for the linear formulation of this model. The impact of this simplification on the obtained results should be negligible as long as  $\Delta t$  is roughly set to the time span of a regular charging process. More importantly, only the queue length is here of relevance, rather than parameters, such as average waiting time, which are estimated using the M/M/\* queuing models.

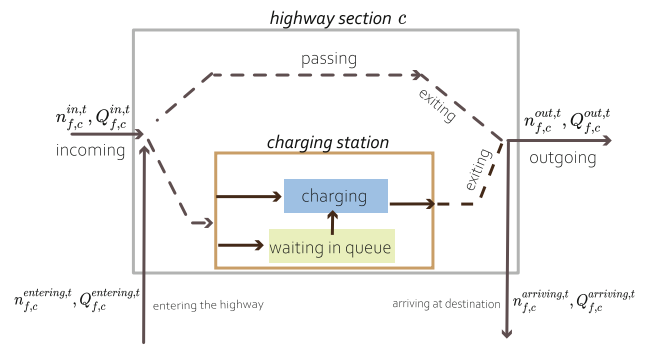


**Fig. 2** Modeled activities of battery electric vehicles at a highway section  $c$ : Vehicles that enter the highway network at highway section  $c$  or travel from an adjacent highway section to this one either pass the charging station here or enter the charging station to charge their battery. If the charging station is fully occupied, vehicles wait in the queue. Subsequently, vehicles travel to the next highway section or arrive at their destination. Next to the number of vehicles of fleet  $f$  at time step  $t$  at each activity,  $n_{f,c}^t$ , their state of charge is also tracked,  $Q_{f,c}^t$

Fig. 2 illustrates how a highway section  $c$  containing a charging station is conceptualized and the different activities of vehicles at a highway section  $c$ : The incoming or outgoing activity describes the movement from one highway section to another. Vehicles enter the highway at the beginning of a highway section and exit the highway network when they reach their destination. Vehicles will either pass by the charging station or enter it, where they will either begin charging immediately or wait in line to charge.

To ensure a minimum state of charge of the vehicles in the fleet  $f$  at all times  $t$  and in all places  $c$ , the state of charge  $Q_{f,c}^t$  is tracked in parallel with the number of vehicles  $n_{f,c}^t$ . For any given time  $t$ , highway section  $c$  and car fleet  $f$ , the number of vehicles  $n_{f,c}^t$  in a specific state is defined together with a charging capacity  $Q_{f,c}^t$ . The following relationship is established between these two layers of information:

$$Q_{f,c}^t \in \left( n_{f,c}^t * SOC^{\min} * Cap_f^{\text{batt}}, n_{f,c}^t * SOC^{\max} * Cap_f^{\text{batt}} \right) \quad (2)$$

$:\forall t, c, f$

These equations ensure that the state of charge is proportional to the number of vehicles at all times and during all vehicle activities. Another important feature introduced by these equations is that the vehicle's state of charge is always high enough for the vehicle to travel further, given a minimum state of charge given in percentage,  $SOC^{\min}$ . Moreover, the battery capacity is not higher than an upper limit of state of charge,  $SOC^{\max}$ , i.e., a vehicle cannot charge more energy than its battery can store when this value is set to 1.

Expressing the movement of the vehicles and the transition between the previously, described activities, constraints in the form of balance equations are defined for both layers of information. For example, the following equation applies for vehicles entering a highway section  $c$  and its state of charge:

$$n_{f,c}^{in,t} + n_{f,c}^{entering,t} = n_{f,c}^{in\_pass,t} + n_{f,c}^{in\_wait\_charge,t} \quad : \forall t, c, f \quad (3)$$

$$Q_{f,c}^{in,t} + Q_{f,c}^{entering,t} = Q_{f,c}^{in\_pass,t} + Q_{f,c}^{in\_wait\_charge,t} \quad : \forall t, c, f \quad (4)$$

The left term,  $n_{f,c}^{in,t} + n_{f,c}^{entering,t}$ , expresses the number of vehicles of a fleet  $f$  entering the highway section  $c$  at time step  $t$ ,  $n_{f,c}^{entering,t}$  being the number of vehicles entering the highway network at time step  $t$  at highway section  $c$  of fleet  $f$  and  $n_{f,c}^{in,t}$  the number of vehicles which have just traveled from an adjacent highway section  $c'$  and entered highway section  $c$ .

The right term,  $n_{f,c}^{in\_pass,t} + n_{f,c}^{in\_wait\_charge,t}$ , represents the split among the fleet, into one part of the fleet  $f$  that is about to pass directly through the highway section  $c$ ,  $n_{f,c}^{in\_pass,t}$ , and another which will proceed to drive to the charging station,  $n_{f,c}^{in\_wait\_charge,t}$ .

The queue itself is modeled analogously to a storage system:

$$n_{f,c}^{wait,t} = n_{f,c}^{wait,t-1} + n_{f,c}^{in\_wait,t} - n_{f,c}^{wait\_charge\_next,t} \quad : \forall t, c, f \quad (5)$$

$$Q_{f,c}^{wait,t} = Q_{f,c}^{wait,t-1} + Q_{f,c}^{in\_wait,t} - Q_{f,c}^{wait\_charge\_next,t} \quad : \forall t, c, f \quad (6)$$

The total number of vehicles waiting in the queue,  $n_{f,c}^{queue,t}$ , is the sum of  $n_{f,c}^{wait,t}$  and  $n_{f,c}^{wait\_charge\_next,t}$ . This number increases when vehicles enter the queue by the amount of  $n_{f,c}^{in\_wait,t}$ . The value decreases at time step  $t+1$  by the number of vehicles that are about to connect to start charging,  $n_{f,c}^{wait\_charge\_next,t}$ .

The energy charged during a charging process by a fleet  $f$  at a time step  $t$ , depends on the number of vehicles charging,  $n_{f,c}^{charge,t}$ , and the charging power of a vehicle,  $\bar{P}_f^{charge, BEV}$ . Moreover, drivers have the flexibility of how long a vehicle is charged which is

bounded by a minimum charging time  $t^{\min}$  and the time resolution  $\Delta t$ <sup>5</sup>:

$$E_{f,c}^{charged,t} \geq n_{f,c}^{charge,t} * \bar{P}_f^{charge, BEV} * t^{\min} * \mu_f^{charge} \quad : \forall t, c, f \quad (7)$$

$$E_{f,c}^{charged,t} \leq n_{f,c}^{charge,t} * \bar{P}_f^{charge, BEV} * \Delta t * \mu_f^{charge} \quad : \forall t, c, f \quad (8)$$

At all charging stations, the total amount of charged energy during each time step  $t$  is limited through the installed capacity at the given highway section  $c$ ,  $Cap_c$ :

$$\sum_f E_{f,c}^{charged,t} * \mu_f^{charge} \leq Cap_c \quad : \forall t, c \quad (9)$$

More details on the mathematical formulation of the model are found in Appendix 2.

### 3.2 Description of Austrian case study

The modeling framework is applied to a fast-charging infrastructure planned for the highway network in the east of Austria. Fig. 3 depicts all highways and motorways within Austrian borders and the geographic extent of the test-bed used for this study. The Austrian highway network can be roughly divided into two unconnected road networks, as shown in this session. The East section of the network has been selected for analysis to present an application to a network that contains multiple intersections and important transit routes throughout of Austria<sup>6</sup>.

Table 1 displays chosen parameter settings for this study's model application. The planned fast-charging infrastructure is designed for the year 2030, a significant year in the decarbonization plans for the transport sector, as the Paris Agreement explicitly

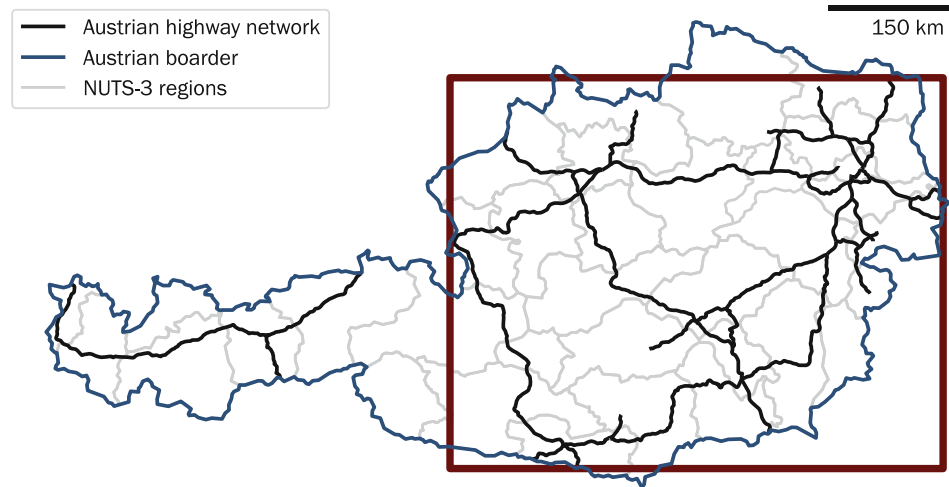
**Table 1** Model parameter settings and characteristics of the modeled battery electric vehicle (BEV) fleet for the application to the test-bed

| Model parameter   | Value       |
|---|-------------|
| Temporal resolution $\Delta t$  | 0.25 h      |
| Driving speed $\nu$   | 110 km/h    |
| BEV share $\epsilon$  | 30%         |
| BEV battery capacity $Cap^{batt}$   | 100 kWh     |
| BEV charging power $\bar{P}^{charge, BEV}$                                    | 250 kW      |
| BEV specific energy consumption at low temperatures $\bar{d}^{spec, winter}$  | 0.2 kWh/km  |
| BEV specific energy consumption at high temperatures $\bar{d}^{spec, summer}$ | 0.15 kWh/km |

<sup>5</sup> Potential restrictions by the electricity grid impacting the electricity grid are neglected and sufficient power supply is assumed here.

<sup>6</sup> For example, parts of this highway network are part of the Rhine-Danube corridor which is essential to the Trans-European Transport Network.

**Fig. 3** Geographical extend of the highway network serving as a test-bed and its allocation in the East of Austria



states a 20% electrification of global road transport by 2030 [32]. The share of electrification in the passenger car fleet is assumed to be higher for Austria than globally, and, therefore, we assume a share of BEVs of 30% in this study, as previously assumed in [11]. The temporal resolution is set to 15 min corresponding to an approximate time of a fast-charging process at 350 kW. Assuming a constant driving speed of 110 km/h in the entire highway network results in a geographic resolution of 27.5 km. Vehicle parameters are set here after predictions and expectations for future developments in BEV technology found in [1, 30].

### 3.2.1 Four representative days

To assess the robustness of a planned charging infrastructure, we observe charging and queuing processes under extreme charging demand conditions. Representative days are created to represent different typical days in traffic load and temperature, as these factors play a vital role in occurrence of charging demand along highways [5, 27, 38]. We include a dif-

**Table 2** Descriptions of representative days used to evaluate the charging infrastructure under different conditions in traffic flow and temperature

| Representative day | Description  |
|--------------------|--|
| Workday in winter  | <ul style="list-style-type: none"> <li>– Travels prominently for the purpose of commuting and business</li> <li>– Cold temperature</li> </ul>  |
| Workday in summer  | <ul style="list-style-type: none"> <li>– Travels prominently for the purpose of commuting and business</li> <li>– Warm temperature</li> </ul>  |
| Holiday in winter  | <ul style="list-style-type: none"> <li>– Travels prominently for the purpose of leisure, increased transit traffic</li> <li>– Increased amount of transit traffic</li> <li>– Cold temperature</li> </ul> |
| Holiday in summer  | <ul style="list-style-type: none"> <li>– Travels prominently for the purpose of leisure, increased transit traffic</li> <li>– Increased amount of transit traffic</li> <li>– Warm temperature</li> </ul> |

ferentiation between workdays and weekend days, commonly made in the description of mobility patterns [5]. Moreover, we introduce these two types of days for a day in both winter and summer and reflect their impact by introducing an increased/decreased specific energy consumption as a result of temperature differences. Table 2 displays a description of the case study. The inclusion of these four case studies aims, among other things, to provide insight into the model's sensitivities to the difference in the distribution of traffic load and temperature.

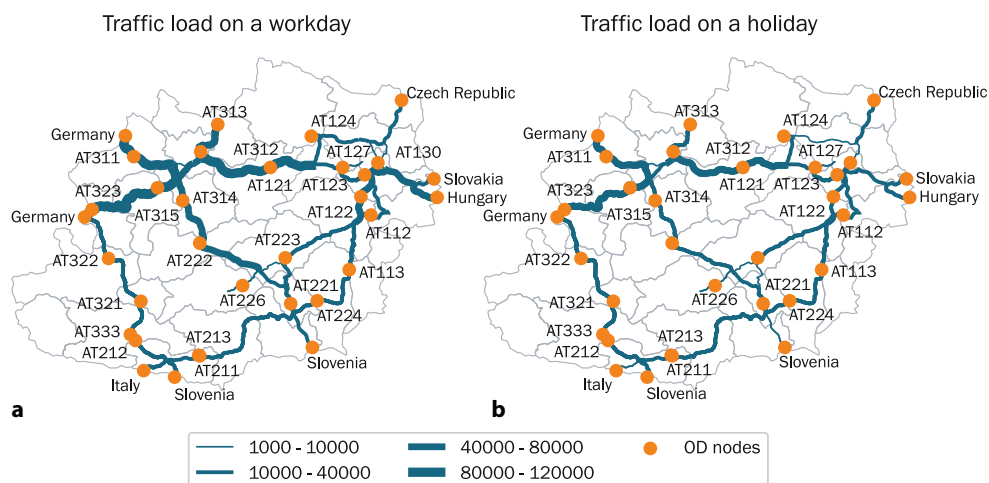
### 3.2.2 Origin-Destination flows

The vehicle movement is defined by the distance between the origin and destination (O–D) nodes on the highway network. For this, O–D points representing NUTS-3 regions are introduced, as well as points representing neighboring countries to include cross-border traffic. Fig. 4 displays these. The position of nodes representing Austrian NUTS-3 regions was determined by projecting the geometric centroids of the most-populated municipality within a region onto the network shape. Nodes representing neighboring countries were placed directly at the network's end points.

The traffic flow data used here describes individual motorized mobility patterns and are obtained from the project *GREENROAD* [4] during which a traffic flow model was calibrated using highway traffic count data for Austria. The data describe the accumulated number of vehicles traveling between Austrian municipalities and neighboring countries on an average workday. Fig. 4 displays the traffic load resulting from long-distance travels and the point allocations of O–D nodes along the Austrian highway network. Based on the traffic load on a workday, traffic load for a typical holiday was derived which is also displayed in Fig. 4.

To dis-aggregate the total daily number of vehicles traveling between the O–D nodes to higher temporal resolution, this study used typical distributions of departure time evaluated in [16]. The temporal res-

**Fig. 4** **a** Traffic load on a workday. **b** Traffic load on a holiday. The orange markers indicate locations of origin–destination (O–D) nodes. Names of the represented countries and NUTS-3 regions are written right beside these



olution of fleets entering the highway network is set to an hour, which means that a certain number of vehicles depart at each full hour at all O–D nodes. We do not anticipate that this resolution will significantly impact the results because movement and charging activities are still observed on a quarter-hourly basis.

### 3.2.3 Input fast-charging infrastructure

Fig. 5 displays the fast-charging infrastructure used here. It is planned for the year 2030 using parameters on the electric vehicle fleet as stated in Table 1 and is the output by a model described in the study by [11]. The planning tool is an optimization model that allocates and sizes fast-charging infrastructure along a high-level road network while keeping infrastructure investment costs to a minimum. It is based on a graph representation of the road network. The

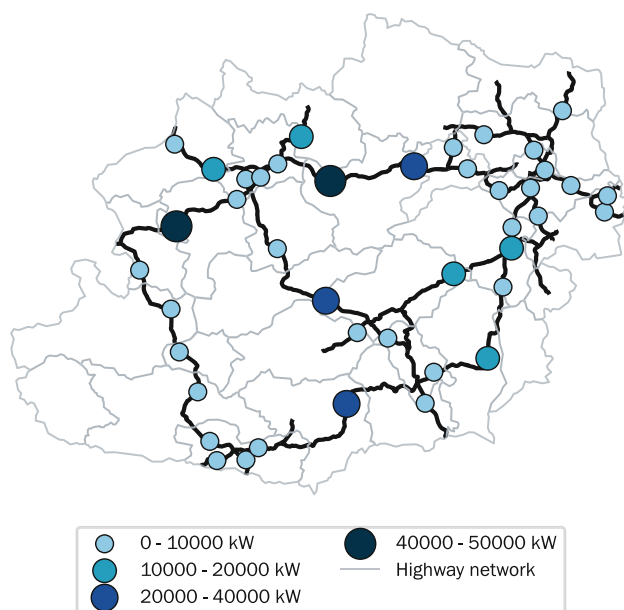


**Fig. 5** Capacities of planned fast-charging infrastructure for 2030

following are the main assumptions and simplifications made in the design of this planning tool:

- For charging station allocation, existing resting areas are considered potential sites, with an upper limit on installed capacity at each.
- Charging demand is defined at each rest stop and is assumed to be the result of the energy consumption of long-distance BEV drivers traveling along the highway network. Here, annual peaks in traffic load and increased energy consumption due to cold temperatures are taken into account. The algorithm determines where charging capacity should be allocated to meet this demand.
- This is done while considering the limited range of BEVs and the geographic distribution of traffic load along the highway network.
- The allocations of origin and destination points of BEVs traveling along the highway network are ignored.

The modeling approach used here for the most part is as described in [11], except for a minor change in the demand calculation for the traffic load resulting from the provided O–D data rather than being retrieved from traffic counters mounted along the highway network.

### 3.3 Open-source programming environment and data availability

The analysis presented here is implemented using Python 3.8 with pyomo 6.2 [14] and Gurobi software [12] for the model solution. The problem size of the case study here is defined by  $|\mathcal{T}| = 120$  observed time steps,  $|\mathcal{C}| = 92$  highway sections and  $|\mathcal{F}| = 700$ . This results in 20 Mio. decision variables and 34 Mio. constraints. Given the large size of this problem, solutions are computed using the barrier algorithm without crossover. The computational time of a model run takes about 1500s for model building and 8000s for the solution on an Intel Core i7 CPU with 3.4GHz



**Table 3** Demand-related descriptors and key performance indicators (KPI) during different representative days

| Metric  | Representative Days |                   |                   |                   |
|---|---------------------|-------------------|-------------------|-------------------|
|   | Workday in winter   | Workday in summer | Holiday in winter | Holiday in summer |
| Total number of long-distance trips   | <b>294,924</b>      | 294,924           | 208,222           | 208,222           |
| Total energy consumed (GWh)   | <b>8.7</b>          | 6.5               | 6.2               | 4.6               |
| Total energy charged by all BEVs (GWh)  | <b>3.3</b>          | 2.8               | 2.7               | 2.3               |
| Avg. state of charge at arrival (%)   | <b>33%</b>          | 35%               | 33%               | 35%               |
| <b>Avg. utility rate UR</b>   | <b>0.52</b>         | 0.48              | 0.47              | 0.43              |
| <b>Avg. difference between peak power and installed capacity <math>\Delta\hat{P}_c</math> in kW (nb. of not used poles)</b> | <b>874 (2–3)</b>    | 1579 (4–5)        | 1672 (4–5)        | 2687 (7–8)        |
| <b>Objective value <math>\sum_{t,f,c} n_{f,c}^{queue,t}</math></b>  | <b>0.0</b>          | 0.0               | 0.0               | 0.0               |

and 64GB RAM. The code is available here: <https://github.com/antoniagolab/StressTestFastChargingInfr>.

## 4 Results

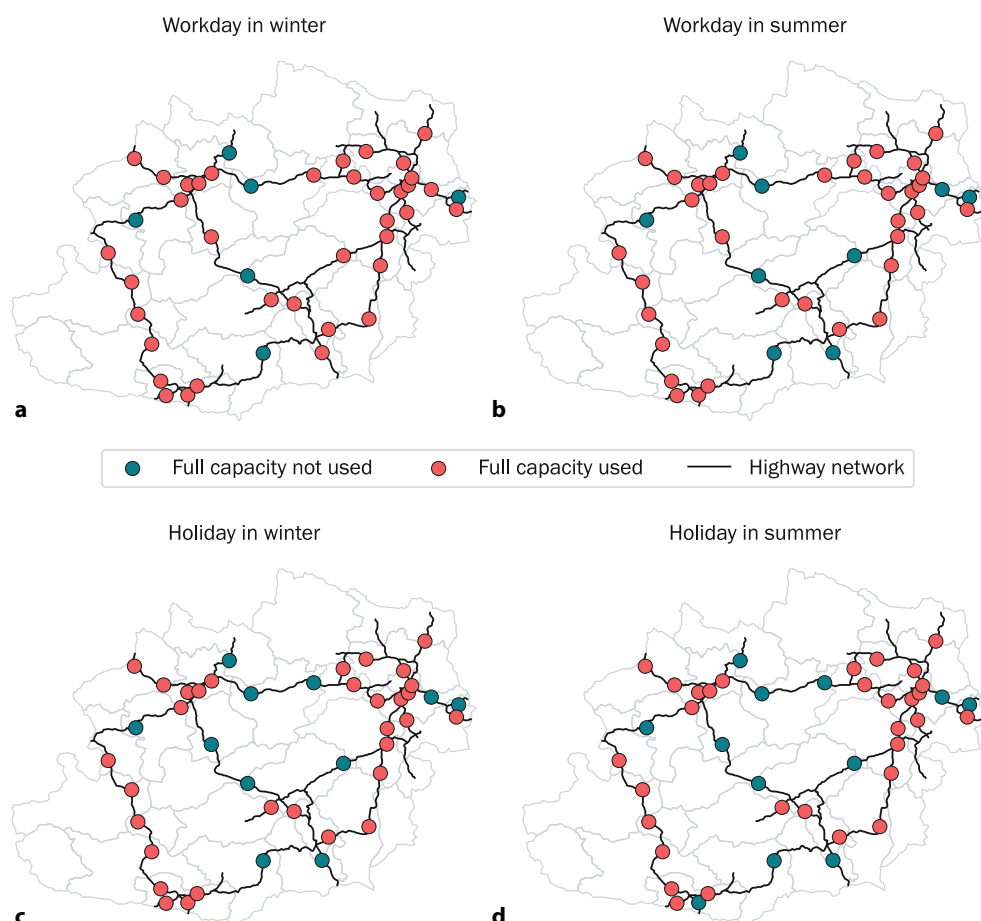
This section presents the most relevant results of this research. First, observations made during model application in the different representative days' conditions are described and compared. The second part of this section takes a closer look at seasonal differences and delves deeper into the operation of two charging stations. Finally, the results of a sensitivity analysis are discussed. The design of this sensitivity analysis is

aimed at observing local changes and changes in the overall charging infrastructure in the response to the removal of charging capacity.

### 4.1 Identification of bottlenecks and overcapacities in planned charging infrastructure

Table 3 displays observations made during the application of the modeling framework to the different representative days which vary in traffic load and temperature. The table displays metrics related to the input to provide insight into the differences in charging demand as well as resulting values for key performance

**Fig. 6** Charging station at which the full capacity is used and not used. Charging stations are classified as fully used if the difference between peak load and installed capacity is smaller than the peak power of a charging pole with 350 kW. Each subfigure displays this classification for a different representative day: **a** Workday in winter. **b** Workday in summer. **c** Holiday in winter. **d** Holiday in summer



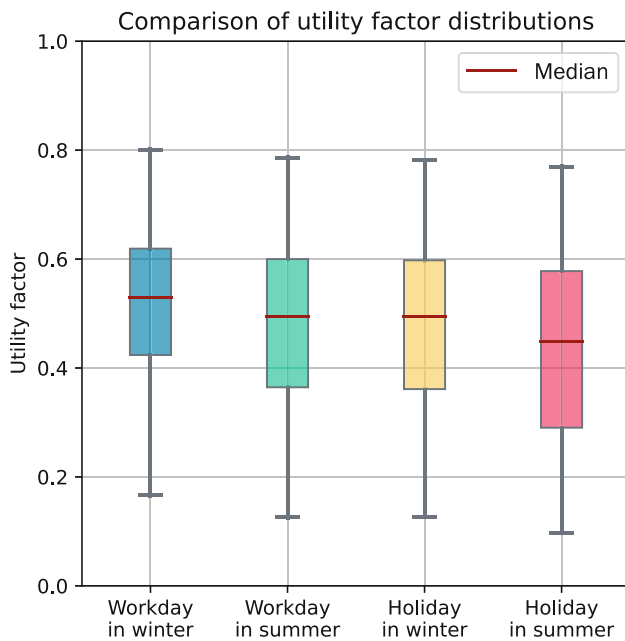


**Fig. 7** Distributions of the utility rate of charging stations during the different representative days

indicators (KPI). Figs. 6 and 7 display more detailed information on the technical KPIs that are the difference between peak load and installed capacity,  $\Delta\hat{P}$ , and the utility rate, UR. Fig. 6 illustrates a binary classification of charging stations, indicating the full local charging capacity at which charging stations are used. Charging stations are classified here as “Full capacity used” when  $\Delta\hat{P}$  is smaller than the peak power of one charging pole, 350 kW, indicating that all charging poles are being used at the given charging station during some point throughout the day. Fig. 7 displays the distributions of the observed values for UR for the four representative days.

Overall, the following observations are made:

- The objective value equals 0 during all days, implying that no queuing occurs in all observed circumstances. Therefore, all battery electric vehicles (BEVs) recharge as soon as they arrive at a charging station, and the considered fast-charging infrastructure has no bottlenecks.
- During the workday in winter, all BEV's total amount of charged energy is the highest which is also reflected by the highest, value of the average UR (0.52). This peak in energy demand is given by the high number of long-distance BEV trips and the increased energy consumption due to the low temperature during winter. The average value for  $\Delta\hat{P}$  is here also the lowest, indicating that, on average, a charging station has 2-3 unused charging poles<sup>7</sup>.
- The state of charge of the vehicles at arrival is slightly higher during the summer workday and

holiday than during the winter. This observation is most likely due to the lower energy consumption of BEVs during the summer.

- The distributions of the utility rates UR do not vary significantly between the representative days as the median and average values vary between 0.43 and 0.56.
- There are six charging stations where none of the observed traffic load and temperature, conditions cause all charging poles to be used. During a summer vacation, the number of charging stations that are not fully utilized increases to 12.

#### 4.2 Insights into infrastructure utilization

Here, a closer look is taken at two charging stations at which significant differences in load occur between the different representative days. Two charging stations were chosen at random from a set of charging stations which are fully utilized during a workday in winter but not on other days (as indicated in Fig. 6). Fig. 8 displays the allocation and load curves of the selected charging stations which are indicated here as “charging station A” and “charging station B”. Table 4 displays observed KPI values for UR and  $\Delta\hat{P}$  to give a more detailed impression on how the local load changes due to the different conditions.

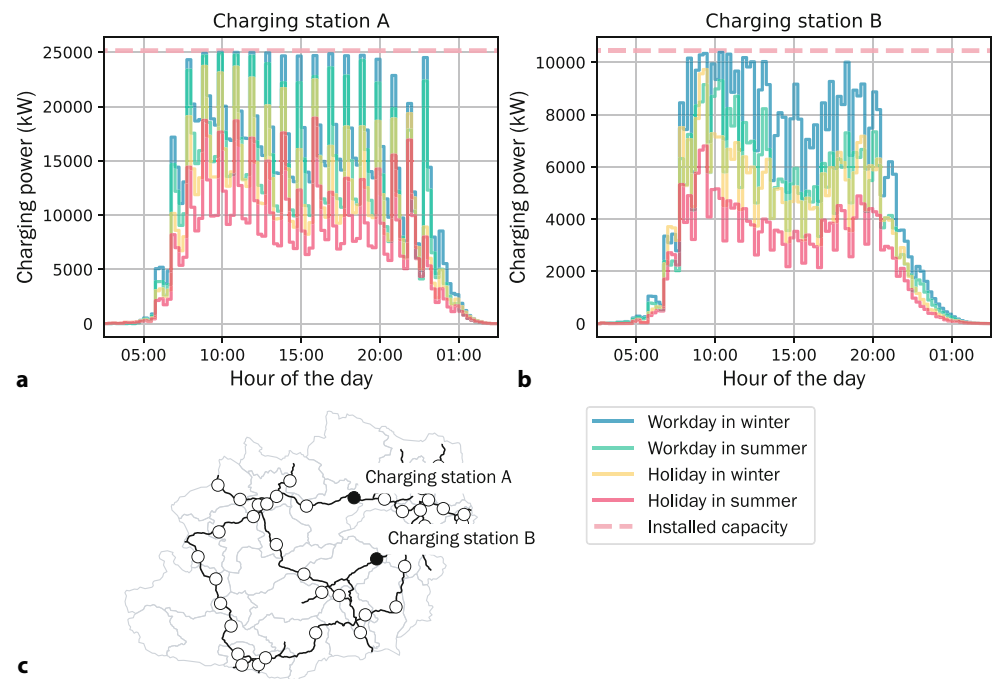
On a holiday in summer, 6212 kW of unused charging capacity at charging station A and 3647 kW at charging station B are observed. This corresponds respectively to 14-15 and 10 unused charging poles. Relative to the total size of the charging stations, this makes up for 25% of all charging capacity at charging station A and 35% at charging station B. On a summer holiday, utilization rate for both charging stations, is cut in half, falling from 0.29 to 0.16 at charging station A and from 0.28 to 0.16 at charging station B. Note that the workday in winter and the holiday in summer represent two extreme conditions in the charging demand and, therefore, they represent such,

**Table 4** Comparison of key performance indicators at two selected charging stations observed during the four different representative days (utility rate UR and the difference between peak load and installed capacity  $\Delta\hat{P}$ )

|                           | Representative days |                   |                   |                   |
|---------------------------|---------------------|-------------------|-------------------|-------------------|
|                           | Workday in winter   | Workday in summer | Holiday in winter | Holiday in summer |
| <i>Charging station A</i> |                     |                   |                   |                   |
| UR                        | 0.29                | 0.24              | 0.22              | 0.16              |
| $\Delta\hat{P}$ (kW)      |                     |                   |                   |                   |
| (nb. of not used poles)   | 154 (0–1)           | 299 (0–1)         | 1456 (4–5)        | 6212 (14–15)      |
| <i>Charging station B</i> |                     |                   |                   |                   |
| UR                        | 0.28                | 0.24              | 0.21              | 0.16              |
| $\Delta\hat{P}$ (kW)      |                     |                   |                   |                   |
| (nb. of not used poles)   | 67 (0–1)            | 1143 (3–4)        | 722 (2)           | 3647 (10–11)      |

<sup>7</sup> Considering a peak power of a charging pole to be 350 kW.

**Fig. 8** **a** Load curves at charging station A observed during the different representative days. **b** Load curves at charging station B observed during the different representative days. **c** Locations of charging stations A and B



the lower and upper limits for a range of charging station utilization.

#### 4.3 Sensitivity analysis: capacity reduction

This sensitivity analysis examines how charging activity changes in response to a capacity reduction in the charging infrastructure. Given that the planning tool used to plan the fast-charging infrastructure allocates charging capacities to cover peak demand, i.e., charging demand on a workday in winter, queuing occurs if charging capacity is reduced. Therefore, we assume that an entire charging station is not operational and thus unavailable for charging.

For this, a charging station annotated as “charging station D” is selected. Its allocation is illustrated in Fig. 9 on the top right. This charging station was chosen for the following reasons: First, it is located on a segment of the highway with multiple charging stations. On a workday in winter, all charging stations on this segment are fully utilized, indicating that no overcapacity exists. Therefore, if a charging station is not operating on this segment, the likelihood of queuing is high because there are no overcapacity facilities nearby to compensate the sudden outage of this charging station. Second, this charging station in particular has the largest capacity sizing along this segment, which again increases the changes that queuing would occur. The load curve of charging station D during a workday in winter is displayed in Fig. 9 on the top left. On a workday in winter, its utility rate is 0.52, whereas 102 MWh is charged here during the total day. Load curves of the directly adjacent charging stations, C and E, are also displayed in Fig. 9

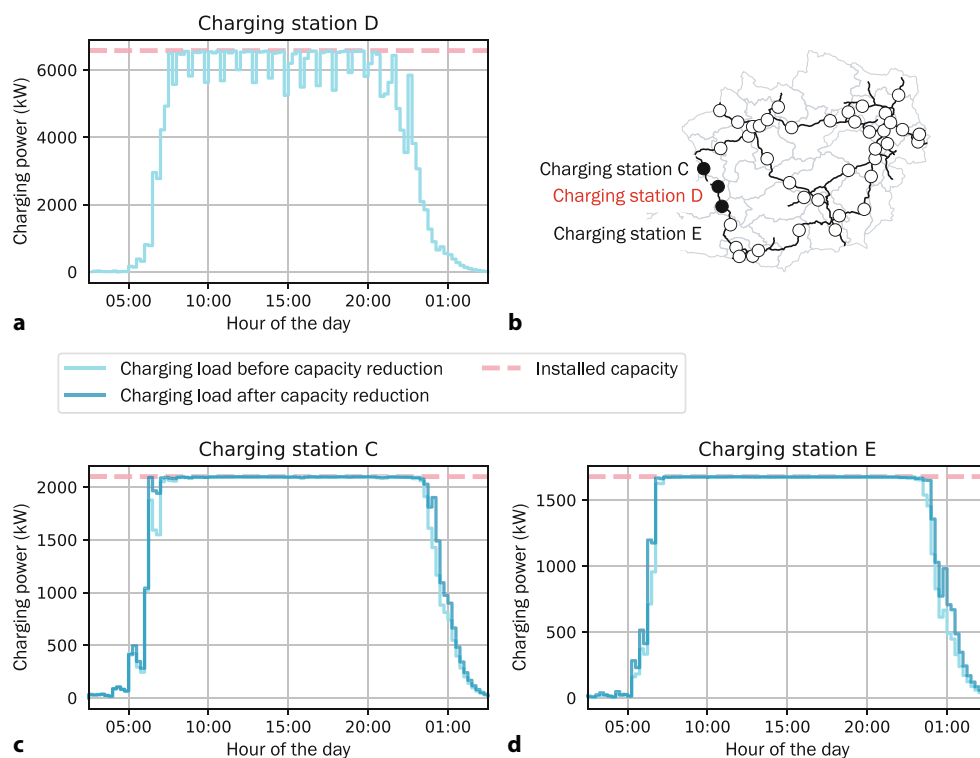
and indicate that these are similarly highly occupied as charging station D.

Table 5 shows how the model output parameters change in response to the capacity reduction at charging station D. Surprisingly, the outage of charging station D does not result in the formation of queues. Overall, the model’s response is unaffected: The state of charge at arrival of all driving BEVs on the highway network and even the ones traveling, including those passing through the highway section where charging station D is located (i.e., likely to charge there) remains consistent. The impact on the load curves of the charging stations C and E is also minor as indicated in Fig. 5 in dark blue. The total amount of the charged energy by all BEVs decreases by 30 MWh and the average UR value increases by 0.01 implying that part of the demand coverage not supplied by charging station D, 102 MWh, is redistributed to other charging stations and compensated through overall slightly higher utilization of the other charging stations in the highway network.

## 5 Discussion

This study’s most striking finding is that no queuing is observed in the charging station network under consideration. A cost-minimizing optimization model allocates and sizes charging capacities based on peak demand to plan the tested fast-charging infrastructure. Peak demand for BEVs typically occurs during a workday in the winter due to high traffic loads and low outdoor temperatures. Moreover, the charging infrastructure under consideration is designed with these specific conditions in mind. Therefore, it is expected that no queuing will occur during the ap-

**Fig. 9** **a** Load curve of charging station D observed during a workday in winter. **b** Locations of charging stations C, D and E. **c** Load curves at charging station C before and after the capacity reduction in charging station D. **d** Load curves at charging station E before and after the capacity reduction in charging station D



**Table 5** Parameters related to charging activity before and after charging capacity is removed from charging station D

|  | Before capacity reduction | After capacity reduction |
|--|---------------------------|--------------------------|
| Total energy charged by all BEVs (MWh)   | 3337                      | 3307                     |
| Av. state of charge at arrival of all vehicles (%)                                 | 32.52%                    | 32.47%                   |
| Av. state of charge at arrival of vehicles traveling through charging station D(%) | 31.64%                    | 31.61%                   |
| Avg. utility rate UR   | 0.52                      | 0.53                     |
| Objective value $\sum_{t,f,c} n_{f,c}^{queue,t}$                                   | 0.0                       | 0.0                      |

plication to all of the considered representative days. Queuing should occur when the demand exceeds peak demand or charging capacity is removed. The latter case is tested during the sensitivity analysis by simulating a charging station outage. Contrary to the expectations, no queuing occurs, and the charging load is compensated at other charging stations throughout the highway network. This implies that the planned charging infrastructure has overestimated charging capacity. This finding is also supported by the presence of large differences in peak load and installed capacity at multiple charging stations on a winter workday. However, the absence of bottlenecks here may be also related to the efficiency of the charging infrastructure modeled by the spatio-temporal charging model.

The accumulation of vehicles into continuous, swarm-like entities most definitely increases this efficiency in charging infrastructure utilization, as the modeled vehicle fleets can split into smaller entities

of arbitrary size, disperse along their route, and redistribute stored energy among them. Like swarm intelligence, this enables the vehicle fleets to act even more efficiently to meet a minimum of the objective function. A more granular representation of vehicles, such as not adding vehicles to a fleet, and defining variables related to the number of vehicles as integers rather than continuous, could help to reduce this “swarm intelligence”. This would substantially increase the problem’s dimension while causing solubility issues, thereby limiting the model’s large-scale applicability. Another factor contributing to this flexibility is the assumption of coordinated charging, which is made in formulating the objective function that is the minimization of the number of vehicles waiting in line. This takes away a BEV driver’s limited individual knowledge of uncoordinated charging and its individual goal of reaching the destination in the shortest amount of time. The assumption of coordinated charging may result in a reduction of peak load because charging activities are organized in such a way that the local peak load at charging stations is reduced to avoid the queue formation.

Based on our thorough analysis and gained experience, we conclude that charging capacities are significantly oversized and partially biased in their position. Possible explanations include the following. First, the charging stations are planned to meet the charging demand expected from long-distance BEVs traveling along the highway network. Therefore, the planned charging infrastructure compensates for all consumed energy. The planning tool ignores the fact that BEVs do not leave the highway network in the same state of



charge that they entered it with. Second, another overlooked piece of information closely related to this is the allocation of the vehicle exit points: Charging demand coverage is partially allocated outside the route of vehicles from which the charging demand originates. Third, the spatial dynamics of demand coverage are taken into account in a limited way overall, whereas the temporal dynamics of charging demand are not considered at all by this planning tool.

## 6 Conclusion

This study tested planned fast-charging capacities in their practical implementation by determining the queuing and waiting time of battery electric vehicles while driving from origin to destination using this infrastructure. By doing so, we contribute to research on a topic that has received little attention thus far. In particular, charging and queuing activities for East Austrian highways in 2030 are investigated under various traffic load conditions. We investigate different representative conditions in traffic load to better understand the use of planned charging capacities. For example, charging and queuing were observed during a winter workday characterized by heavy traffic and increased energy consumption of BEVs due to low temperatures. Overall, there was no queuing; thus, no bottlenecks were identified in this charging infrastructure. Nonetheless, high utilization was observed at many charging stations. Meanwhile, spare charging capacity that was never used was detected at other charging stations during peak demand on a winter workday. This implies a charging capacity missallocation. The obtained results on utilization factors and peak load, as well as the insights into seasonal differences in charging activity, can aid in gaining a better understanding of the economics of a fast-charging station allocated at a rest area along a highway.

Our findings also point to the importance of including spatio-temporal dynamics in the planning of fast-charging infrastructure, that is, how charging activities change in response to changes in charging capacity, most notably expansion. The observed response in our results is to some degree impacted by the assumption of coordinated charging. In this regard, future research should be investigate the impact of charging infrastructure expansion on charger utilization given less coordination of the charging activity. Aside from the assumption of coordinated charging, other model formulation simplifications must be tested for their impact on observed results in smaller test-beds, such as the representation of groups of vehicles as continuous entities and the coarse representation of the charging and waiting processes determined by the chosen size of observed time steps.

Furthermore, more insight into how a planning tool can be improved to meet charging demand while allocating charging infrastructure cost-efficiently is required. The proposed implementability test can pro-

vide information on allocating potential bottlenecks and spare capacity under various temperature and traffic load conditions. The next step is to create a modeling framework that will allow these insights to be built upon and parameters describing flaws in the planned infrastructure to be fed back into a planning tool. This approach may combine a top-down with a bottom-up methodology, allowing both benefits.

**Acknowledgements** The authors acknowledge TU Wien Bibliothek for financial support for proofreading and through its Open Access Funding Program. Moreover, the authors are thankful to TRAFFIX Verkehrsplanung GmbH for providing the traffic flow data of Austria.

**Funding** Open access funding provided by TU Wien (TUW).

**Open Access** This article is licensed under a Creative Commons Attribution 4.0 International License, which permits use, sharing, adaptation, distribution and reproduction in any medium or format, as long as you give appropriate credit to the original author(s) and the source, provide a link to the Creative Commons licence, and indicate if changes were made. The images or other third party material in this article are included in the article's Creative Commons licence, unless indicated otherwise in a credit line to the material. If material is not included in the article's Creative Commons licence and your intended use is not permitted by statutory regulation or exceeds the permitted use, you will need to obtain permission directly from the copyright holder. To view a copy of this licence, visit <http://creativecommons.org/licenses/by/4.0/>.

## 7 Appendix

### 7.1 Nomenclature

**Table 6** Nomenclature

| Nomenclature                             |   |
|--|---|
| <i>Indices</i>                           |   |
| $t \in \mathcal{T}$                      | Time step   |
| $c \in \mathcal{C}$                      | Highway section   |
| $f \in \mathcal{F}$                      | Vehicle fleet   |
| <i>Decision variables</i>                |   |
| $n_{f,c}^{\text{in},t}$                  | Number of incoming vehicles of fleet $f$ to highway section $c$ at time step $t$  |
| $Q_{f,c}^{\text{in},t}$                  | (kWh) stored energy in batteries of incoming fleet $f$ to highway section $c$ at time step $t$                          |
| $n_{f,c}^{\text{pass},t}$                | Number of vehicles of fleet $f$ which drive through highway section $c$ at time step $t$                                |
| $Q_{f,c}^{\text{pass},t}$                | (kWh) stored energy in batteries of fleet $f$ passing through highway section $c$ at time step $t$                      |
| $n_{f,c}^{\text{queue},t}$               | Number vehicles of fleet $f$ in queue at highway section $c$ at time step $t$   |
| $Q_{f,c}^{\text{queue},t}$               | (kWh) stored energy in batteries of fleet $f$ that is waiting in queue at highway section $c$ at time step $t$          |
| $n_{f,c}^{\text{entering},t}$            | Number of vehicles of fleet $f$ which enter the highway network at highway section $c$ at time step $t$                 |
| $Q_{f,c}^{\text{entering},t}$            | (kWh) stored energy in batteries of fleet $f$ which enter the highway network at highway section $c$ at time step $t$   |
| $n_{f,c}^{\text{arriving},t}$            | Number of vehicles of fleet $f$ which arrive at their destination at highway section $c$ at time step $t$               |
| $Q_{f,c}^{\text{arriving},t}$            | (kWh) stored energy in batteries of fleet $f$ which arrive at their destination at highway section $c$ at time step $t$ |
| $n_{f,c}^{\text{charge},t}$              | Number of vehicles of fleet $f$ charging at highway section $c$ at time step $t$  |
| $E_{f,c}^{\text{charged},t}$             | (kWh) energy charged by vehicles of fleet $f$ at highway section $c$ at time step $t$                                   |
| <i>Technical vehicle fleet specifics</i> |   |
| $Q_f^{\text{init}}$                      | (kWh) initial state of charge at departure of fleet $f$   |
| $\bar{d}_f^{\text{spec}}$                | (kWh/km) average specific energy consumption of car fleet $f$   |
| $\bar{P}_f^{\text{charge,BEV}}$          | (kW) average charging power of car fleet $f$  |
| $\mu_f^{\text{charge}}$                  | Charging efficiency of fleet $f$  |
| $\text{Cap}_f^{\text{batt}}$             | (kWh) battery charging capacity of fleet $f$  |
| $\text{SOC}_f^{\text{init}}$             | (%) state of charge of fleet $f$ at the entrance to the highway network   |
| $\text{SOC}^{\text{min}}$                | (%) minimum allowed state of charge of a BEV battery  |
| $\text{SOC}^{\text{max}}$                | (%) maximum allowed state of charge of a BEV battery  |
| <i>Infrastructure-related parameters</i> |   |
| $\text{Cap}_c$                           | (kW) installed charging capacity at highway section $c$   |
| $\text{dist}_c$                          | (km) length of highway section $c$  |
| $\text{UR}_c$                            | Utilization rate of charging station allocated at highway section $c$   |
| $\Delta \hat{P}_c$                       | (kW) difference between peak load and installed capacity at charging station located at highway section $c$             |

## 7.2 Details on mathematical formulation of spatio-temporal charging

Further equations of the charging model are described in the following. Tables 7 and 8 provide descriptions on the variables and formulas.

$$Q_{f,c}^{\text{entering},t} = n_{f,c}^{\text{entering},t} * \text{SOC}_f^{\text{init}} * \text{Cap}_f^{\text{batt}} \quad (10)$$

$$n_{f,c}^{\text{in\_wait\_charge},t} = n_{f,c}^{\text{in\_wait},t} + n_{f,c}^{\text{in\_charge},t} \quad (11)$$

$$Q_{f,c}^{\text{in\_wait\_charge},t} = Q_{f,c}^{\text{in\_wait},t} + Q_{f,c}^{\text{in\_charge},t} - E_{f,c}^{\text{consumed\_charge\_wait},t} \quad (12)$$

$$E_{f,c}^{\text{consumed\_charge\_wait},t} = \frac{1}{2} * \text{dist}_c * \bar{d}_f^{\text{spec}} * n_{f,c}^{\text{in\_charge},t} \quad (13)$$

$$n_{f,c}^{\text{to\_charge},t} = n_{f,c}^{\text{in\_charge},t} + n_{f,c}^{\text{wait\_charge\_next},t-1} \quad (14)$$

$$n_{f,c}^{\text{charge}1,t} = n_{f,c}^{\text{in\_charge},t} \quad (15)$$

$$Q_{f,c}^{\text{input\_charge}1,t} = Q_{f,c}^{\text{in\_charge},t} \quad (16)$$

$$n_{f,c}^{\text{charge}1,t} = n_{f,c}^{\text{output\_charged}1,t} \quad (17)$$

$$n_{f,c}^{\text{output\_charged}1,t+1} = n_{f,c}^{\text{finished\_charge}1,t} + n_{f,c}^{\text{charge}2,t} \quad (18)$$

$$Q_{f,c}^{\text{output\_charged}1,t+1} = Q_{f,c}^{\text{input\_charge}1,t} + E_{f,c}^{\text{charged}1,t} \quad (19)$$

$$Q_{f,c}^{\text{output\_charged}1,t} = Q_{f,c}^{\text{input\_charge}2,t} + Q_{f,c}^{\text{finished\_charge}1,t} \quad (20)$$

$$n_{f,c}^{\text{output\_charged}2,t+1} = n_{f,c}^{\text{finished\_charge}2,t} + n_{f,c}^{\text{charge}3,t} \quad (21)$$

$$Q_{f,c}^{\text{output\_charged}2,t+1} = Q_{f,c}^{\text{input\_charge}2,t} + E_{f,c}^{\text{charged}2,t} \quad (22)$$

$$Q_{f,c}^{\text{output\_charged}2,t} = Q_{f,c}^{\text{input\_charge}3,t} + Q_{f,c}^{\text{finished\_charge}2,t} \quad (23)$$

$$n_{f,c}^{\text{output\_charged}3,t+1} = n_{f,c}^{\text{finished\_charge}3,t} \quad (24)$$

$$Q_{f,c}^{\text{output\_charged}3,t+1} = Q_{f,c}^{\text{input\_charge}3,t} + E_{f,c}^{\text{charged}3,t} \quad (25)$$

$$Q_{f,c}^{\text{output\_charged}3,t} = Q_{f,c}^{\text{finished\_charge}3,t} \quad (26)$$

$$n_{f,c}^{\text{finished\_charge},t} = n_{f,c}^{\text{finished\_charge}1,t} + n_{f,c}^{\text{finished\_charge}2,t} + n_{f,c}^{\text{finished\_charge}3,t} \quad (27)$$

$$Q_{f,c}^{\text{finished\_charge},t} = Q_{f,c}^{\text{finished\_charge}1,t} + Q_{f,c}^{\text{finished\_charge}2,t} + Q_{f,c}^{\text{finished\_charge}3,t} \quad (28)$$

$$n_{f,c}^{\text{exit},t+1} = n_{f,c}^{\text{pass},t} + n_{f,c}^{\text{finished\_charge},t} \quad (29)$$

$$Q_{f,c}^{\text{exit},t+1} = Q_{f,c}^{\text{pass},t} + Q_{f,c}^{\text{finished\_charge},t} - E_{f,c}^{\text{consumed\_pass},t} - E_{f,c}^{\text{consumed\_exit\_charge},t} \quad (30)$$

$$E_{f,c}^{\text{consumed\_pass},t} = \text{dist}_c * \bar{d}_f^{\text{spec}} * n_{f,c}^{\text{pass},t} \quad (31)$$

$$E_{f,c}^{\text{consumed\_exit\_charge},t} = \frac{1}{2} * \text{dist}_c * \bar{d}_f^{\text{spec}} * n_{f,c}^{\text{finished\_charge},t} \quad (32)$$

$$n_{f,c}^{\text{exit}} = n_{f,c}^{\text{arriving},t} + n_{f,c}^{\text{out},t} \quad (33)$$

$$Q_{f,c}^{\text{exit}} = Q_{f,c}^{\text{arriving},t} + Q_{f,c}^{\text{out},t} \quad (34)$$

$$n_{f,c}^{\text{out},t} = n_{f,c}^{\text{in},t} \quad (35)$$

**Table 7** Complementary nomenclature

| Decision variables                      |  |
|---|--|
| $n_{f,c}^{\text{wait},t}$               | Number of vehicles of fleet $f$ which wait in queue at highway section $c$ at time step $t$ and will not leave it at time step $t + 1$   |
| $Q_{f,c}^{\text{wait},t}$               | (kWh) stored energy in batteries of vehicles of fleet $f$ which wait in queue at highway section $c$ at time step $t$ and will not leave it at time step $t + 1$                       |
| $n_{f,c}^{\text{in\_wait\_charge},t}$   | Number of vehicles of fleet $f$ which are about to enter the charging station and proceed to charge or wait in queue at highway section $c$ at time step $t$                           |
| $Q_{f,c}^{\text{in\_wait\_charge},t}$   | (kWh) stored energy in batteries of vehicles of fleet $f$ which are about to enter the charging station and proceed to charge or wait in queue at highway section $c$ at time step $t$ |
| $n_{f,c}^{\text{in\_wait},t}$           | Number of vehicles of fleet $f$ which are about to enter the queue at highway section $c$ at time step $t$   |
| $Q_{f,c}^{\text{in\_wait},t}$           | (kWh) stored energy in batteries of vehicles of fleet $f$ which are about to enter the queue at highway section $c$ at time step $t$   |
| $n_{f,c}^{\text{in\_pass},t}$           | Number of vehicles of fleet $f$ which are about to pass through highway section $c$ at time step $t$   |
| $Q_{f,c}^{\text{in\_pass},t}$           | (kWh) stored energy in batteries of vehicles of fleet $f$ which are about to pass through highway section $c$ at time step $t$   |
| $n_{f,c}^{\text{in\_charge},t}$         | Number of vehicles of fleet $f$ which are about to charge at highway section $c$ at time step $t$  |
| $Q_{f,c}^{\text{in\_charge},t}$         | (kWh) stored energy in batteries of vehicles of fleet $f$ which are about to charge at highway section $c$ at time step $t$  |
| $n_{f,c}^{\text{to\_charge},t}$         | (kWh) number of vehicles of fleet $f$ which are entering the charging station without waiting in the queue at highway section $c$ at time step $t$                                     |
| $n_{f,c}^{\text{wait\_charge\_next},t}$ | Number of vehicles of fleet $f$ which are about to enter the charging station but are still in the queue at highway section $c$ at time step $t$                                       |
| $n_{f,c}^{\text{charge}1,t}$            | Number of vehicles of fleet $f$ charging at highway section $c$ at time step $t$ during first time span of $\Delta t$  |
| $n_{f,c}^{\text{charge}2,t}$            | Number of vehicles of fleet $f$ charging at highway section $c$ at time step $t$ during second time span of $\Delta t$   |
| $n_{f,c}^{\text{charge}3,t}$            | Number of vehicles of fleet $f$ charging at highway section $c$ at time step $t$ during third time span of $\Delta t$  |

Table 7 (Continued)

| Decision variables                          |  |
|---|--|
| $Q_{f,c}^{\text{input\_charge}1,t}$         | (kWh) stored energy in batteries of vehicles of fleet $f$ before entering the charging station at highway section $c$ at time step $t$   |
| $Q_{f,c}^{\text{output\_charge}1,t}$        | (kWh) stored energy in batteries of vehicles of fleet $f$ after charging for the time span of $\Delta t$ the charging station at highway section $c$ at time step $t$                    |
| $Q_{f,c}^{\text{input\_charge}2,t}$         | (kWh) stored energy in batteries of vehicles of fleet $f$ before starting to charge for the time span of another $\Delta t$ at highway section $c$ at time step $t$                      |
| $Q_{f,c}^{\text{output\_charge}2,t}$        | (kWh) stored energy in batteries of vehicles of fleet $f$ after charging for the time span of $2 * \Delta t$ at the charging station at highway section $c$ at time step $t$             |
| $Q_{f,c}^{\text{input\_charge}3,t}$         | (kWh) stored energy in batteries of vehicles of fleet $f$ before starting to charge for the time span of a third $\Delta t$ at highway section $c$ at time step $t$                      |
| $Q_{f,c}^{\text{output\_charge}3,t}$        | (kWh) stored energy in batteries of vehicles of fleet $f$ after charging for the time span of $3 * \Delta t$ at the charging station at highway section $c$ at time step $t$             |
| $n_{f,c}^{\text{finished\_charge}1,t}$      | Number of vehicles of fleet $f$ charging at highway section $c$ at time step $t$ which are finished with the charging after first time span of $\Delta t$                                |
| $n_{f,c}^{\text{finished\_charge}2,t}$      | Number of vehicles of fleet $f$ charging at highway section $c$ at time step $t$ which are finished with the charging after time span $2 * \Delta t$                                     |
| $n_{f,c}^{\text{finished\_charge}3,t}$      | Number of vehicles of fleet $f$ charging at highway section $c$ at time step $t$ which are finished with the charging after time span $3 * \Delta t$                                     |
| $Q_{f,c}^{\text{finished\_charge}1,t}$      | (kWh) stored energy in batteries of vehicles of fleet $f$ after finishing charging after the time span of $1 * \Delta t$ at the charging station at highway section $c$ at time step $t$ |
| $Q_{f,c}^{\text{finished\_charge}2,t}$      | (kWh) stored energy in batteries of vehicles of fleet $f$ after finishing charging after the time span of $2 * \Delta t$ at the charging station at highway section $c$ at time step $t$ |
| $Q_{f,c}^{\text{finished\_charge}3,t}$      | (kWh) stored energy in batteries of vehicles of fleet $f$ after finishing charging after the time span of $3 * \Delta t$ at the charging station at highway section $c$ at time step $t$ |
| $n_{f,c}^{\text{finished\_charge},t}$       | Number of vehicles of fleet $f$ which are finished charging at highway section $c$ at time step $t$  |
| $Q_{f,c}^{\text{finished\_charge},t}$       | (kWh) stored energy in batteries of vehicles of fleet $f$ after finishing charging at the charging station at highway section $c$ at time step $t$                                       |
| $n_{f,c}^{\text{exit},t}$                   | Number of vehicles of fleet $f$ which are leaving highway section $c$ at time step $t$   |
| $Q_{f,c}^{\text{exit},t}$                   | (kWh) stored energy in batteries of vehicles of fleet $f$ which are leaving highway section $c$ at time step $t$   |
| $n_{f,c}^{\text{out},t}$                    | Number of vehicles of fleet $f$ which are leaving highway section $c$ but not the highway network at time step $t$   |
| $Q_{f,c}^{\text{out},t}$                    | (kWh) stored energy in batteries of vehicles of fleet $f$ which are leaving highway section $c$ but not the highway network at time step $t$   |
| $E_{f,c}^{\text{consumed\_charge\_wait},t}$ | (kWh) energy consumed by vehicles of fleet $f$ which are about to enter the charging station or queue at highway section $c$ at time step $t$  |
| $E_{f,c}^{\text{consumed\_exit\_charge},t}$ | (kWh) energy consumed by vehicles of fleet $f$ which have charged and are about to exit highway section $c$ at time step $t$   |
| $E_{f,c}^{\text{consumed\_pass},t}$         | (kWh) energy consumed by vehicles of fleet $f$ which have passed highway section $c$ at time step $t$  |

Table 8 Formula descriptions

| Formula reference | Description  |
|-------------------|--|
| A1                | Definition of initial state of charge of vehicles entering the highway section   |
| A2, A3, A4        | The charging station is placed at the middle of a highway section where the vehicles proceed to directly charge or wait in queue.  |
| A5, A6            | The number of charging vehicles consists of the ones that directly proceed to charging after entering the charging station and the ones exiting the queue.   |
| A7–A19            | Vehicles can charge up to the time span of $3 * \Delta t$ which corresponds in the case study of this work to 45 min. This model feature was implemented here to allow vehicles of the charging power of down to 44 kW also allow to charge as charging at this power is classified as the lowest power for fast-charging. |
| A9, A12, A15      | After each $\Delta t$ , vehicles may be either finished with the charging process or proceed to charge for another $\Delta t$ . This is limited to $3 * \Delta t$  |
| A20–A23           | Energy is consumed while driving through a highway section and between finishing charging at a charging station and exiting the highway section.   |
| A24, A25, A26     | At the end point of a highway section, vehicles either exit the highway network as they have reached their destination or enter the next highway section that is along their route.  |



## References

- Andersen PB et al (2019) Innovation outlook: Smart charging for electric vehicles. Int Renew Energy Agency. [https://www.irena.org/-/media/Files/IRENA/Agency/Publication/2019/May/IRENA\\_Innovation\\_Outlook\\_EV\\_smart\\_charging\\_2019.pdf](https://www.irena.org/-/media/Files/IRENA/Agency/Publication/2019/May/IRENA_Innovation_Outlook_EV_smart_charging_2019.pdf). Accessed 20 July 2022
- Bae S, Kwassinski A (2012) Spatial and temporal model of electric vehicle charging demand. *IEEE Trans Smart Grid* 3(1):394–403. <https://doi.org/10.1109/TSG.2011.2159278>
- Bireselioglu ME, Demirbag Kaplan M, Yilmaz BK (2018) Electric mobility in europe: A comprehensive review of motivators and barriers in decision making processes. *Transportation Res Part A: Policy Pract* 109:1–13. <https://doi.org/10.1016/j.tra.2018.01.017> (<https://www.sciencedirect.com/science/article/pii/S0965856417311771>)
- BMK (2022) Verkehrsmodell. <https://www.bmk.gv.at/themen/verkehrsplanung/verkehrsmodell.html>. Accessed 19 July 2022
- BMK (2014) Österreich unterwegs 2013/2014. <https://www.bmk.gv.at/themen/verkehrsplanung/statistik/oesterreich-unterwegs.html>. Accessed 27 Jan 2022
- Coffman M, Bernstein P, Wee S (2017) Electric vehicles revisited: a review of factors that affect adoption. *Transport Rev* 37(1):79–93. <https://doi.org/10.1080/01441647.2016.1217282>
- Csiszár C, Csonka B, Földes D, Wirth E, Lovas T (2019) Location optimisation method for fast-charging stations along national roads. *J Transp Geogr* 88(May):966–992. <https://doi.org/10.1016/j.jtrangeo.2020.102833>
- Daina N, Sivakumar A, Polak JW (2017) Modelling electric vehicles use: a survey on the methods. *Renew Sustain Energy Rev* 68:447–460. <https://doi.org/10.1016/j.rser.2016.10.005>
- Frei A, Kuhnimhof TG, Axhausen KW (2010) Long distance travel in europe today: Experiences with a new survey. *Arbeitsberichte Verkehrs- und Raumplanung*, vol 611
- Ghamami M, Zockaie A, Nie YM (2016) A general corridor model for designing plug-in electric vehicle charging infrastructure to support intercity travel. *transportation Res Part C: Emerg Technol* 68:389–402. <https://doi.org/10.1016/j.trc.2016.04.016>
- Golab A, Zwickl-Bernhard S, Auer H (2022) Minimum-cost fast-charging infrastructure planning for electric vehicles along the austrian high-level road network. *Energies*. <https://doi.org/10.3390/en15062147> (<https://www.mdpi.com/1996-1073/15/6/2147>)
- Gurobi Optimization (2022) Gurobi Optimizer Reference Manual. <https://www.gurobi.com>. Accessed 20 July 2022
- Hamedmoghadam H, Jalili M, Vu HL, Stone L (2021) Percolation of heterogeneous flows uncovers the bottlenecks of infrastructure networks. *Nat Commun* 12(1):1–10
- Hart WE, Watson J-P, Woodruff DL (2011) Pyomo: modeling and solving mathematical programs in python. *Math Program Comput* 3(3):219–260
- Helmus JR, Lees MH, van den Hoed R (2022) A validated agent-based model for stress testing charging infrastructure utilization. *Transportation Res Part A: Policy Pract* 159:237–262. <https://doi.org/10.1016/j.tra.2022.03.028>
- Hiesl A, Ramsebner J, Haas R (2021) Modelling stochastic electricity demand of electric vehicles based on traffic surveys—the case of austria. *Energies*. <https://doi.org/10.3390/en14061577> (<https://www.mdpi.com/1996-1073/14/6/1577>)
- Hodgson MJ (1990) A flow-capturing location-allocation model. *Geogr Anal* 22(3):270–279
- Hu L, Dong J, Lin Z (2019) Modeling charging behavior of battery electric vehicle drivers: A cumulative prospect theory based approach. *Transportation Res Part C: Emerg Technol* 102:474–489. <https://doi.org/10.1016/j.trc.2019.03.027>
- Jochem P, Szimba E, Reuter-Oppermann M (2019) How many fast-charging stations do we need along European highways? *Transportation Res Part D: Transport Environ* 73(January):120–129. <https://doi.org/10.1016/j.trd.2019.06.005>
- Kavianipour M, Fakharmoosavi F, Shojaei MH, Zockaie A, Ghamami M, Wang J, Jackson R (2021) Impacts of technology advancements on electric vehicle charging infrastructure configuration: a Michigan case study. *Int J Sustain Transportation* 0(0):1–14. <https://doi.org/10.1080/15568318.2021.1914789>
- Kuby M, Lim S (2005) The flow-refueling location problem for alternative-fuel vehicles. *Socioecon Plann Sci* 39(2):125–145. <https://doi.org/10.1016/j.seps.2004.03.001>
- Lindgren J, Lund PD (2015) Identifying bottlenecks in charging infrastructure of plug-in hybrid electric vehicles through agent-based traffic simulation. *Int J Low-carbon Technol* 10(2):1748–1317. <https://doi.org/10.1093/ijlct/ctv008>
- Metais MO, Jouini O, Perez Y, Berrada J, Suomalainen E (2022) Too much or not enough? Planning electric vehicle charging infrastructure: A review of modeling options. *Renew Sustain Energy Rev* 153(November 2020):111719. <https://doi.org/10.1016/j.rser.2021.111719>
- Mu Y, Wu J, Jenkins N, Hongjie J, Wang C (2014) A spatial-temporal model for grid impact analysis of plug-in electric vehicles. *Appl Energy* 114:456–465. <https://doi.org/10.1016/j.apenergy.2013.10.006>
- Napoli G, Polimeni A, Micari S, Andaloro L, Antonucci V (2020) Optimal allocation of electric vehicle charging stations in a highway network: Part I. Methodology and test application. *J Energy Storage* 201(April):101102. <https://doi.org/10.1016/j.est.2019.101102>
- Pagany R, Ramirez Camargo L, Dorner W (2019) A review of spatial localization methodologies for the electric vehicle charging infrastructure. *Int J Sustain Transportation* 13(6):433–449. <https://doi.org/10.1080/15568318.2018.1481243>
- Splawińska M (2017) Factors determining seasonal variations in traffic volumes. *Arch Civ Eng*. <https://doi.org/10.1515/ace-2017-0039>
- Spöttle M, Jörling K, Schimmel M, Staats M, Grizzell L, Jerram L, Drier W, Gartner J (2018) Research for TRAN Committee—Charging infrastructure for electric road vehicles (European Parliament)
- Suarez C, Martinez W (2019) Fast and Ultra-Fast Charging for Battery Electric Vehicles—A Review. *Ieee Energy Convers Congr Expo 2019*(2019):569–575. <https://doi.org/10.1109/ECCE.2019.8912594>
- Thielmann A, Wietschel M, Funke S, Grimm A, Hettesheimer T, Langkau S, Loibl A, Moll C, Neef C, Plötz P, Sievers L, Espinoza LT, Edler J (2020) Batterien für Elektroautos: Faktencheck und Handlungsbedarf. *Perspektiven – Policy Brief*, vol 01 (<https://hdl.handle.net/10419/233461>)
- Ul-Haq A, Marium A, Mahmoud Y, Aqib P, Al-Amr EA (2017) Probabilistic modeling of electric vehicle charging pattern associated with residential load for voltage unbalance assessment. *Energies* 10(9):1996–1073. <https://doi.org/10.3390/en10091351> (<https://www.mdpi.com/1996-1073/10/9/1351>)
- United Nations Framework Convention on Climate Change. Paris declaration on electro-mobility and climate change and call to action. *epub*, 2015.

33. Upchurch C, Kuby M, Lim S (2009) A model for location of capacitated alternative-fuel stations. *Geogr Anal* 41(1):85–106. <https://doi.org/10.1111/j.1538-4632.2009.00744.x>
34. Wang Y, Jianmai S, Wang R, Liu Z, Wang L (2018) Siting and sizing of fast charging stations in highway network with budget constraint. *Appl Energy* 228:1255–1271. <https://doi.org/10.1016/j.apenergy.2018.07.025>
35. Xie F, Lin Z (2021) Integrated u.s. nationwide corridor charging infrastructure planning for mass electrification of intercity trips. *Appl Energy* 298(0306261921005821):117142. <https://doi.org/10.1016/j.apenergy.2021.117142>
36. Xie R, Wei W, Khodayar ME, Wang J, Mei S (2018) Planning fully renewable powered charging stations on highways: A data-driven robust optimization approach. *Ieee Trans Transport Electric* 4(3):817–830
37. Yue XD, Cao LB, Miao DQ, Chen YF, Xu B (2015) Multi-view attribute reduction model for traffic bottleneck analysis. *Knowl Based Syst* 86(0950705115001161):1–10. <https://doi.org/10.1016/j.knosys.2015.03.022>
38. Yuksel T, Michalek JJ (2015) Effects of regional temperature on electric vehicle efficiency, range, and emissions in the united states. *Environ Sci Technol* 49(6):3974–3980
39. Zhili Zhou, Lin T (2012) Spatial and temporal model for electric vehicle rapid charging demand. *IEEE Veh Power Propuls Conf Pages*. <https://doi.org/10.1109/VPPC.2012.6422675>

**Publisher's Note** Springer Nature remains neutral with regard to jurisdictional claims in published maps and institutional affiliations.



**Antonia Golab**, joined the Energy Economics Group (EEG) as a university assistant and PhD candidate in May 2021. Already during her studies in Geodesy and Geoinformation at TU Wien she has gained experience in teaching as a tutor and teaching assistant in the associated bachelor and master programme. During her studies, she spent a semester abroad at ETH Zürich which led her to pursue a specialization in the field of Geoinformation. After

finishing her studies she decided to bring in her expertise as a PhD candidate at EEG in the field of energy system analysis with high spatial resolution and high granularity of energy/transport network infrastructure representation. In particular, she focuses on spatial energy infrastructure capacity modeling in the transport sector in general, and the high-level road network infrastructure in particular.



**Sebastian Zwickl-Bernhard**, is a research associate and PhD candidate at the Energy Economics Group (EEG). He joined EEG already in 2018 as a teaching assistant and after graduating in Electrical Engineering (Energy Systems and Automation Engineering) at TU Wien in 2020, he started his PhD studies. At EEG, Sebastian significantly contributes in research to open source modelling and scientific publishing in renowned journals. He also is strongly involved in

teaching and the supervision of bachelor and master students. His expertise is in open source modeling of energy systems with a high spatial granularity and energy network representation. He is involved in different national and European projects, focusing in particular on techno-economic trade-offs and optimal decision trajectories in energy systems to achieve the medium-term (“Fit-for-55”) and long-term climate targets (“1.5°C climate target”).



**Theresia Perger**, is a research assistant and PhD candidate at the Institute of Energy Systems and Electric Drives in the Department of Energy Economics at the Vienna University of Technology. She completed her bachelor's degree in electrical engineering and information technology as well as the master's program in energy and automation technology at the Vienna University of Technology. She is currently working in the field of energy markets, specialized in

local energy communities and local electricity markets. In her position as a university assistant, her work includes teaching various master courses in energy economics and energy modeling, and supervision of master theses.



**Hans Auer**, is an Associate Professor in Energy Economics at TU Wien. He received a M.Sc. in Electrical Engineering (1996), a PhD (2000) and a Venia Docendi (2012) in Energy Economics from TU Wien. Hans joined the Energy Economics Group (EEG) in 1995 and was on research leave several times (e.g., TU Berlin, Lawrence Berkeley National Laboratory, Massachusetts Institute of Technology). Since the beginning of his academic career, Hans has

been focusing on various aspects of energy system modelling and energy system decarbonization, notably in the context of grid and market integration of renewable energy technologies as well as energy sector coupling at several granularity levels. In the last 25 years, Hans has been coordinating a series of European and national projects in the energy transition field for a variety of different clients. He has comprehensive teaching, supervision, reviewing and examination experience of bachelor, master and PhD students, a significant amount of energy conferences contributions worldwide and also authored more than 100 peer-reviewed scientific papers and book contributions. He is an active member in different academic and scientific committees and associations.